Evaluation of the protectiveness of an organosilane coating on patinated Cu-Si-Mn bronze for contemporary art

Giulia Masi, Claudie Josse, Jérôme Esvan, Cristina Chiavari, Elena Bernardi, Carla Martini, Maria Chiara Bignozzi, Cecilia Monticelli, Federica Zanotto, Andrea Balbo, et al.

Evaluation of the protectiveness of an organosilane coating on patinated Cu-Si-Mn bronze for contemporary art

G. Masi[a,*], C. Josse[b], J. Esvan[c], C. Chiavari[d], E. Bernardi[e], C. Martini[f], M.C. Bignozzi[a], C. Monticelli[g,h], F. Zanotto[g,h], A. Balbo[g,h], E. Svara Fabjan[i], T. Kosec[i], L. Robbiola[j]

[a] Dipartimento di Ingegneria Civile, Chimica, Ambientale e dei Materiali, Università di Bologna, via Terracini 28, 40131, Bologna, Italy
[b] Centre de Microcaractérisation Raimond Castaing (CNRS UMS 3623), Université Fédérale de Toulouse, 31400, Toulouse, France
[c] Centre Interuniversitaire de Recherche et d'Ingénierie des Matériaux, Université de Toulouse, 4 allée Emile Monso, 31030, Toulouse, France
[d] Dipartimento di Beni Culturali, Università di Bologna, Italy
[e] Dipartimento di Chimica Industriale "Toso Montanari", Università di Bologna, viale del Risorgimento 4, 40136, Bologna, Italy
[f] Dipartimento di Ingegneria Industriale, Università di Bologna, viale del Risorgimento 4, 40136, Bologna, Italy
[g] Centro di Studi sulla Corrosione e Metallurgia "A. Daccò", Università di Ferrara, Ferrara, Italy
[h] Tecnopolo di Ferrara, Rete dell'Alta Tecnologia della Regione Emilia Romagna, Italy
[i] Slovenian National Building and Civil Engineering Institute, Dimičeva 12, SI-1000, Ljubljana, Slovenia
[j] TRACES Lab (CNRS UMR5608), Université Toulouse Jean-Jaurès, S, allées Antonio-Machado, 31058, Toulouse, France

ARTICLE INFO

Keywords:
Organic coating
Bronze
Atmospheric corrosion
UV degradation
Electrochemical techniques
XPS

ABSTRACT

A 3-mercapto-propyl-trimethoxysilane coating (PropS-SH) applied on Cu-Si-Mn bronze, patinated by "liver of sulphur", was investigated as a non-toxic alternative to Incralac®, usually applied on outdoor artistic bronzes. Electrochemical testing was performed in synthetic acid rain. Exposure to temperature/UV cycles and accelerated corrosion test simulating unsheltered exposure to rainwater was also carried out. The exposed samples were characterised by FEG-SEM coupled with EDS on FIB cross-sections and XPS on free surfaces. The black patina without protective coating was scarcely protective against bronze corrosion and easily transformed into cuprous oxide. PropS-SH coating fully preserved the black patina microstructure and phase constituents (cuprous oxide and cuprous sulphide). The PropS-SH coating also resulted more protective than Incralac® when aged under run-off conditions. Selective dissolution of copper from the silicon bronze alloy was observed on both uncoated and Incralac®-coated bronze, leading to the formation of an internal Si-rich corrosion layer.

1. Introduction

Protection of outdoor bronze monuments has been attracting a significant research interest since the restoration programme of the Quadriga of the Basilica di San Marco in Venice in 1977, which is a cornerstone event in the field of cultural heritage conservation [1]. Protective treatments, including both cleaning procedures and application of surface coatings, such as acrylic polymers admixed with corrosion inhibitors (Incralac®), were found to be the best solution against atmospheric corrosion [1].

Incralac® was developed in 1964 by the International Copper Research Association (INCRA) [2]. It is an unpatented formulation based on Acryloid B 44, a thermoplastic methyl methacrylate copolymer manufactured by Rohm and Haas, dissolved in rather toxic solvents, like toluene and xylene [3]. Incralac® also contains benzotriazole (BTA) as a copper corrosion inhibitor and chelating agent (suspected of carcinogenicity [4]), together with a levelling agent (either Paraplex G 60, which is epoxidized soybean oil, or a silicone oil). BTA also acts as a coating UV stabilizer [5].

Following this approach, micro crystalline wax and other organic polymers, such as poly siloxanes, were later developed [5 9]. Among the others, 3 mercapto propyl trimethoxysilane (PropS SH) proved to be effective for the protection of bare Cu and Cu based alloys in NaCl solution [10 13], as well as in synthetic acid rain [14]. The protectiveness of PropS SH is enhanced by the addition of nanoparticles [15]. In previous works, PropS SH was applied on quaternary bronze, pre

*Corresponding author.
E-mail addresses: giulia.masi5@unibo.it (G. Masi), claudie.josse@ums-castaing.fr (C. Josse), jerome.esvan@ensiacet.fr (J. Esvan), cristina.chiavari@unibo.it (C. Chiavari), elena.bernardi@unibo.it (E. Bernardi), carla.martini@unibo.it (C. Martini), maria.bignozzi@unibo.it (M. CBignozzi), cecilia.monticelli@unife.it (C. Monticelli), federica.zanotto@unife.it (F. Zanotto), andrea.balbo@unife.it (A. Balbo), erika.svara-fabjan@zag.si (E. Svara Fabjan), tadeja.kosec@zag.si (T. Kosec), luc.robbiola@univ-tlse2.fr (L. Robbiola).

https://doi.org/10.1016/j.porgcoat.2018.11.027

patinated by dropping test simulating the exposure to acid rain run off [16,17]. PropS SH can form, after hydrolysis in hydroalcoholic solu tion, metalsiloxane (Me−O−Si) [18] and/or metal thiolate (Me−S−C) bonds [19], ensuring strong adherence to the substrate. It also exhibits good performance against bronze corrosion during subsequent drop ping exposures [17].

Several investigations about the protectiveness of innovative coat ings have been performed, mainly related to traditional casting bronze, involving ternary or quaternary alloys (Cu Sn Zn Pb) [14,20 23]. However, the development of industrial copper based alloys led to less toxic, lead free materials for artistic bronze foundry. Traditional casting, either by lost wax process or by sand casting, is currently carried out also using modern Cu Si Mn alloys. Due to its excellent corrosion resistance, good weldability, remarkable castability and golden colour, this silicon bronze is now widely used by artistic foun dries for bronze monuments [24].

Usually bronzes exposed in outdoor conditions are patinated to improve both aesthetical features and corrosion resistance [25]. Black patination, historically based on the use of *Barèges* salt during the 19th century, has been further developed with the use of K_2S aqueous so lution applied by cold or hot techniques [25 27]. Recent investigations showed that the traditional black patina on pure copper and bronze varies not only with the metallic substrate but also with temperature, as a function of the adopted application techniques [26,27]. The torch (hot) technique was the most common method used by 19th century bronze *patineurs* and still remains a basic process in cultural heritage for architectural and ornamental applications of Cu based alloys. It is still used today for large bronze sculptures [25,26]. To our knowledge, no published reports investigated the protective efficiency of coatings on modern artistic bronze (Cu Si Mn), artificially patinated with tradi tional recipes and exposed to atmospheric conditions.

Therefore, with the final aim of improving the corrosion resistance of patinated modern bronze exposed to outdoor conditions and of preserving the nature and microstructure of the patina, this research focuses on assessing the protective efficiency of a silane coating PropS SH onto K_2S patinated modern cast bronze (CuSi3Mn). In particular, PropS SH has been assessed as a possible alternative to Incralac® (which has a higher impact on health and environment).

Preliminary screening of the coatings performance was firstly car ried out by electrochemical tests. However, the electrochemical ap proach does not provide information on the surface evolution as a function of outdoor exposure conditions [14,28,29]. Therefore, a complementary assessment was subsequently carried out, based on a specific accelerated corrosion test (dropping test), closely simulating unsheltered exposure to rainwater [16]. The release of metallic cations in the ageing solution was quantified, in order to identify the possible influence of alloying elements on the corrosion behaviour. Moreover, complementary analytical methods were applied, involving colori metric measurements as well as X ray photoelectron spectroscopy (XPS), grazing angle X ray diffraction (GXRD) and FEG SEM (Field Emission Gun Scanning Electron Microscope) observation of *in situ* cross sections, prepared by Focused Ion Beam (FIB) milling. This characterisation allowed to correlate coating behaviour with surface evolution.

2. Materials and methods

2.1. Materials

2.1.1. Bronze alloy

The bronze, supplied by Livartis Foundry d.o.o, Slovenia (www.livartis.si/en), is an as cast silicon manganese alloy (Cu Si Mn), with 3.1 ± 0.4 Si and 0.9 ± 0.1 Mn (wt%) as main alloying elements, also containing Sn and Zn (< 0.1 wt%) and P (0.02 wt%) as trace elements. It corresponds to the copper casting alloy UNS C87300 [30]. As cast plates (5 mm thick) were obtained by sand casting. Metallographic examination (not shown in this paper) revealed a typical dendritic microstructure with Si coring and a few shrinkage cavities within in terdendritic spaces. CuSi3Mn plates were cut to obtain 25 × 25 (for dropping and spectroscopic tests) or 50 × 50 mm^2 (for electrochemical tests) coupons.

2.1.2. Patina application

Traditional black patina was applied on the bronze coupons by the torch technique [25 27,31]. The patination process was performed by Livartis Foundry, according to the good practice of artistic foundries. Before patination, coupons were sandblasted over the as cast surfaces. Sand blasting procedure was executed by Kärcher HD 1080 machine at pressure 230 bar and Termit quartz sand with granulation 0.063 0.71 mm, using water flow rate at 800 L/h. The bronze surface was then preheated with a torch up to 50 60 °C and an aqueous solution of po tassium sulphide (K_2S, Merck, p.a. quality at 3 wt.%) was applied by brushing until a black colour appeared. Heating and application cycles were repeated until the typical black colour was fully developed and, finally, the metal was allowed to dry and rinsed with tap water. The free surface of K_2S patinated bronze was analysed by Glow Discharge Op tical Emission Spectroscopy (GD OES). The concentration profiles were measured after gentle rinsing with ethanol, so as to remove surface contamination. GD OES analysis was carried out with a Grimm style glow discharge lamp in DC mode, as detailed in [32].

2.1.3. Preparation and application of tested coatings

3 Mercapto propyl trimethoxy silane (PropS SH, purity 95%, Aldrich) was dissolved in a hydroalcoholic solution (90/5/5 v/v ethanol/water/PropS SH), acidified to pH 4 by addition of some drops of diluted sulphuric acid solution, according to a coating preparation methodology tuned during previous tests [12,14,19,21]. After 24 h hydrolysis at room temperature, the solution was used for coating preparation. Incralac® was purchased from Bresciani s.r.l. (www.brescianisrl.it) and was used both undiluted (dip coating application method) and as a 3 wt% solution in ethyl acetate solvent (solution often adopted by restorers, here used in the case of the spraying application method).

For both PropS SH and Incralac®, dip coating consisted of 1 h im mersion in the coating formulation, followed by fast withdrawal. Subsequently, the coatings were cured at 50 °C for 24 h, before exposure to the aggressive environments. This application method produced si lane and Incralac® films with different final specific weights (about 1.6 g m^{-2} and 5.6 g m^{-2} on average, respectively) and thus with different thicknesses. Therefore, in order to compare the protective efficiency of coatings under similar conditions, a spraying application method (fol lowed by 24 h curing at 50 °C) was also applied, producing coatings with a constant specific weight of 6 ± 1 g m^{-2}. The latter application method has the further advantage to be more consistent with the cur rent practices adopted by conservators.

Contact angle measurements were determined by static method, using FTA 1000 DropShape Instrument B FrameSystem, First Ten Angstroms. The droplet of distilled water (4 μL) was placed on the solid surface and the image was recorded. Contact angle was defined by fitting Young Laplace equation.

2.2. Protective assessment of coatings

Black patinated samples in the as supplied condition (henceforward “uncoated”) and black patinated bronze coated by Incralac® or PropS SH were investigated using several experimental techniques, described in the following paragraphs.

2.2.1. Electrochemical evaluation

In order to achieve accelerated corrosion conditions, the electro chemical tests (EIS and ohmic drop compensated polarization curves) were performed in a tenfold concentrated synthetic acid rain solution

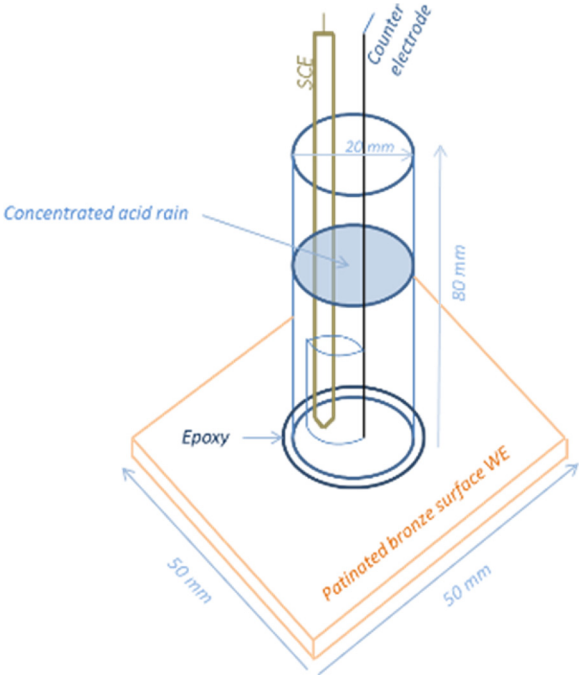

Fig. 1. Electrochemical cell for the preliminary assessment of coating protectiveness.

(ARx10, pH 3.30). The non concentrated rain solution (AR) reproduced the composition of winter acid rains collected over 2001 2003 in Bologna (Italy) and was used as a reference for similar studies [16,22,28,33]. AR was synthetized following the recipe reported in [23] and the ion concentrations were: SO_4^{2-} 1.90 mg L^{-1}, Cl 1.27 mg L^{-1}, NO_3 4.62 mg L^{-1}, CH_3COO 0.23 mg L^{-1}, HCOO 0.05 mg L^{-1}, NH_4^+ 1.05 mg L^{-1}, Ca^{2+} 0.34 mg L^{-1}, Na^+ 0.53 mg L^{-1}, pH 4.35. Sigma Aldrich ACS reagents and HNO_3 65% Merck suprapur were used.

The electrochemical cell consisted of a poly methyl methacrylate tube with internal diameter of 20 mm and height of 80 mm, which was glued onto 50 × 50 × 5 mm^3 uncoated or coated bronze coupons by an epoxy adhesive (Fig. 1).

In this tube, filled by ARX10, a Pt wire and a saturated calomel electrode (SCE) were introduced to act as counter and reference electrodes respectively, while the bronze specimen underneath was the working electrode for electrochemical measurements.

With the aim to limit the effects of water evaporation (leading to solution concentration) and pH variation due to the corrosion process (pH increase connected to oxygen reduction), the ARX10 solution was renewed after 1, 2 and 3 weeks (168, 336 and 504 h), just after the scheduled electrochemical measurements. The tests were performed by a PAR/ AMETEK PARSTAT2273 potentiostat/galvanostat.

The evolution of the bronze corrosion process was monitored over 30 days of exposure by electrochemical impedance spectroscopy (EIS), under the following experimental conditions: ± 10 mV rms alternating potential signal with respect to the corrosion potential (E_{cor}), 100 kHz 1 mHz frequency range and 10 frequencies/decade. Polarization resistance (R_p) values were estimated from the spectra in the Nyquist form, as the difference between the limit of the real part of the impedance at frequency tending to 0 (R_p'), and the solution resistance (R_s) value, that is $R_p = R_p' - R_s$. The time evolution over time of the R_p and E_{cor} average were obtained by triplicate experiments.

Ohmic drop compensated polarization curves were collected after 1 h, 24 h and 30 days of immersion. Separate anodic and cathodic potential scans, always starting from E_{cor}, were carried out at a rate of 0.1667 mV s^{-1}. These tests were performed in triplicate and representative curves are reported. The corrosion protection efficiency, PE, was calculated according to Eq. (1):

$$PE = \frac{J_{cor0} - J_{cor}}{J_{cor0}} \times 100 \quad (1)$$

where J_{cor0} is the value for the uncoated sample and J_{cor} is the corrosion current density for protected surfaces. The corrosion current densities were obtained by the Tafel extrapolation from the polarization curves. All the potentials quoted in the text are related to the SCE reference electrode.

2.2.2. Climatic chamber exposure with temperature/UV cycles and colour measurements

The sprayed PropS SH coating was tested in climatic chamber. As plain PropS SH coatings are known to undergo degradation due to exposure to temperature/UV cycles in climatic chamber [14], these samples were prepared with a silane formulation also containing a commercial anti UV product (8 wt% vs PropS SH of TINUVIN® 400 by BASF). This option was taken into account for assessing the possibility to pre industrialize the PropS SH coating formulation for outdoor applications.

The test procedure for evaluating UV protection efficiency was performed using two climatic chambers: Q sun Xe 3 test chamber, Q lab and climatic chamber KK 340 CHLT, Kambič, for obtaining the defined UV freezing conditions, respectively.

The exposure consisted of 17 cycles, corresponding to 3 average months of UV exposure in the natural conditions. Each cycle consisted of four steps:

Step 1: 2 h temperature ramp (from 0 °C to 35 °C, first cycle from room temperature to 35 °C, UV light switched off),

Step 2: 16 h of UV exposure part (UV light switched on, UV irradiance 55 W m^{-2}, T 35 °C and relative humidity 70%),

Step 3: 2 h temperature ramp (from 35 °C to 0 °C, UV light switched off) and

Step 4: 4 h of freezing (4 h at 0 °C, UV light switched off).

All the samples were characterized by visual observation before and after exposure to UV and temperature cycles, as well as by the measurement of the colour coordinates in the CIELab colour space on the uncovered surface of the samples in three different areas. The measurement of colour coordinates in the same areas on the surface samples (before and after the exposure) was achieved by using an adjustable frame. These measurements were carried out by using a Datacolor D400 spectrophotometer with a D65 illuminant, a 10° observer, a measured area of ∅ 6.6 mm and specular component excluded (SCE), operating with a d/0 SCE measuring geometry. In the CIELab space, each colour is defined by three coordinates: L*, corresponding to lightness and ranging from 0 (black) to 100 (white), a* and b*, corresponding to the chromatic coordinates and without specific numerical limits (+a* is red, a* green, +b* yellow, b* blue). Total colour change (ΔE*) was calculated through Equation (2):

$$\Delta E^* = \sqrt{(\Delta L^*)^2 + (\Delta a^*)^2 + (\Delta b^*)^2} \quad (2)$$

For each sample, ΔE* was calculated by averaging the ΔE* of the three measured areas.

In general, ΔE* values lower than 3 can be assumed as not appreciable and, in the field of Cultural Heritage, ΔE* in the range between 3 and 5 are considered acceptable, while ΔE* > 5 are considered clearly perceivable [34].

2.2.3. Ageing method: dropping test

In order to evaluate the specific impact of outdoor conditions, accelerated ageing was carried out by the dropping test, closely simulating unsheltered geometries directly exposed to rainwater [16]. Cycles of exposure to weathering solution were carried out on both uncoated and coated samples by spraying. Only one side (25 × 25 mm) of each coupon was directly exposed to the weathering solution, while the other surfaces were protected by epoxy resin. For this ageing test, the weathering solution was the non concentrated acid rain solution

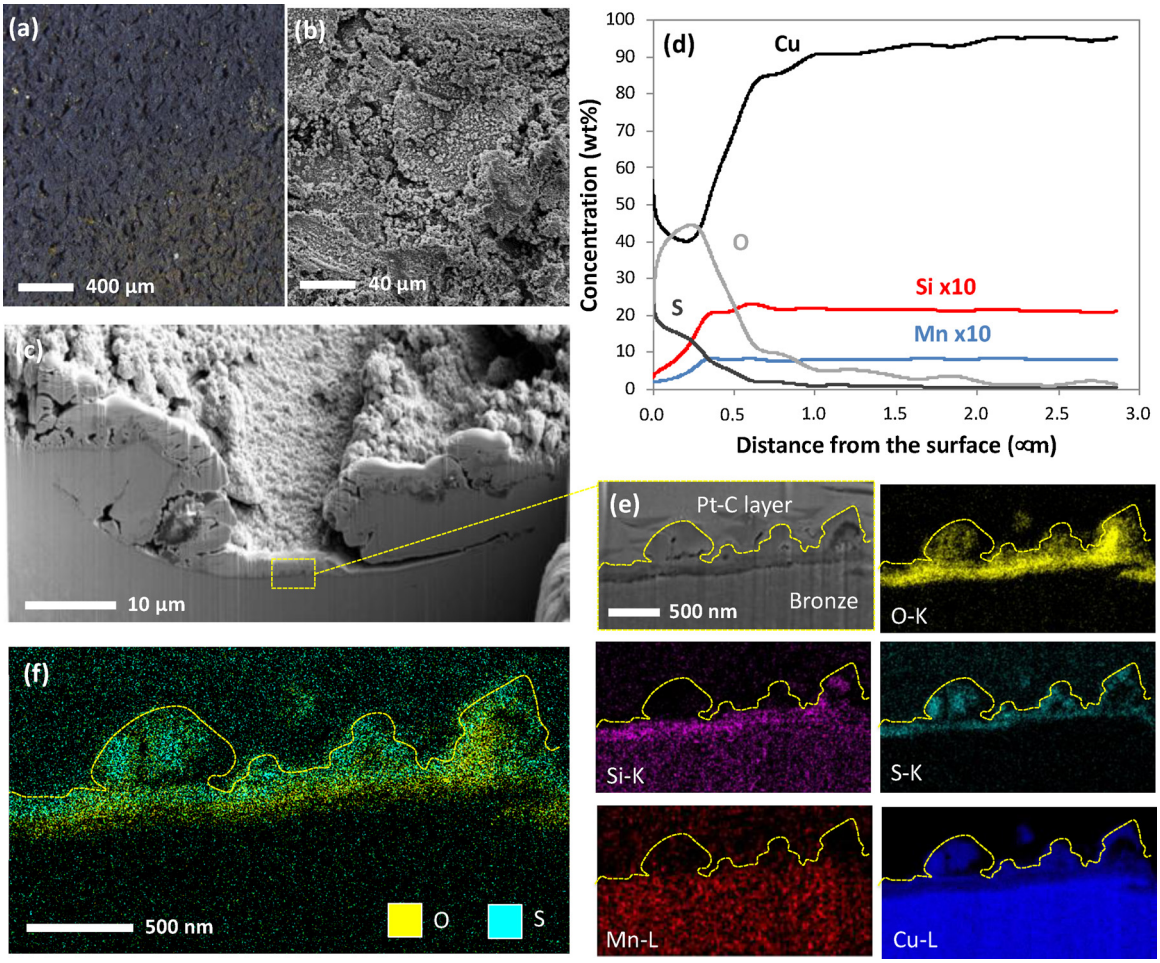

Fig. 2. Morphology of "as-supplied" black patina (K_2S) on CuSi3Mn bronze: (a) optical image of the black patina; (b) general view of the patina surface; (c) in situ FIB cross-section of a representative portion of the sample; (d) GD-OES concentration profiles of S and alloying elements (Cu, Si and Mn) measured as a function of the distance from the free surface. In order to improve the readability of the image, the GD-OES concentration profiles for Si and Mn were amplified 10 times (x10). (e) X-ray maps (C, O, Si, S, Cu) of the black patina; (f) superimposition of O (yellow) and S (cyan) EDS signal to highlight the layered structure of the patina (For interpretation of the references to colour in this figure legend, the reader is referred to the web version of this article).

(AR, Section 2.2.1).

The dropping test [16] consisted of periods of AR dropping onto the samples and periods of sample drying. In particular, cycles of 3 days of dropping / 1 day drying and 2 days of dropping / 1 day drying were alternated for two weeks, reaching a total Time of Wetness (ToW) of 10 days per sample. Duplicate experiments were performed simultaneously for each surface condition. All the samples were placed at a 45° angle on polytetrafluoroethylene supports. A peristaltic pump dropped the AR solution by means of four capillary tubes per sample, with an almost constant dropped volume of 60 mL h^{-1} on each exposed sample. The runoff solution was separately collected from each sample. At the end of each dropping period, volume and pH of the collected solutions were recorded. Then, samples of the solutions were placed in HDPE bottles, acidified with HNO_3 65% suprapur (to prevent adsorption of cations on the bottle surfaces and favour dissolution of any metal complex) and stored at 4 °C for the subsequent analysis of the released metal cations (Cu, Mn and Si). The concentration of Cu and Mn in the weathering solutions was determined through Atomic Absorption Spectrometry (AAS), by using a Perkin Elmer AAnalyst 400 provided with Flame Atomization and a Perkin Elmer PinAAcle 900Z and with Transversely Heated and longitudinal Zeeman background correction. The latter instrument reaches a Limit of Detection of 0.3 µg L^{-1} for Cu and 0.2 µg L^{-1} for Mn. Si concentration was measured by Microwave Plasma Atomic Emission Spectrometer (MP AES) Agilent 4210 with a Limit of Detection of 18 µg L^{-1}. Due to the leaching effect of dropping, that hinders the growth of corrosion products, the protective efficiency of the tested coatings was quantified through metal release in the ageing solutions. In particular, the Inhibiting Efficiency in terms of metal release (η_M) was calculated using Eq. (3):

$$\eta_M = \left(\frac{M_{sol,NC} - M_{sol,C}}{M_{sol,NC}} \right) \times 100 \quad (3)$$

where M_{sol} is the amount of metal released in the ageing solution per aged surface unit (µg cm^{-2}); *NC* is the uncoated sample and *C* is the coated sample, as reported in [35].

In addition, at the end of each dry period, gravimetric measure ments were carried out by a digital balance KERN AGB210 4 with re peatability of ± 0.1 mg. The mass variation during exposure tests was calculated as the difference between the initial weight of the sample and the weight of the samples at different ageing times.

2.2.4. *Surface analysis and structural characterization*

After the colorimetric measurements, all the samples were char acterised by Scanning Electron Microscopy (SEM) coupled with Energy Dispersive Spectroscopy (EDS), X ray diffraction under grazing angle (GXRD) and by X ray photoelectron spectroscopy (XPS).

The colorimetric measurements were carried out on samples before and after coating application, as previously described in Section 2.2.2. At least three samples were used for calculating average values of colour variations (ΔL*, Δa*, Δb*, ΔE*).

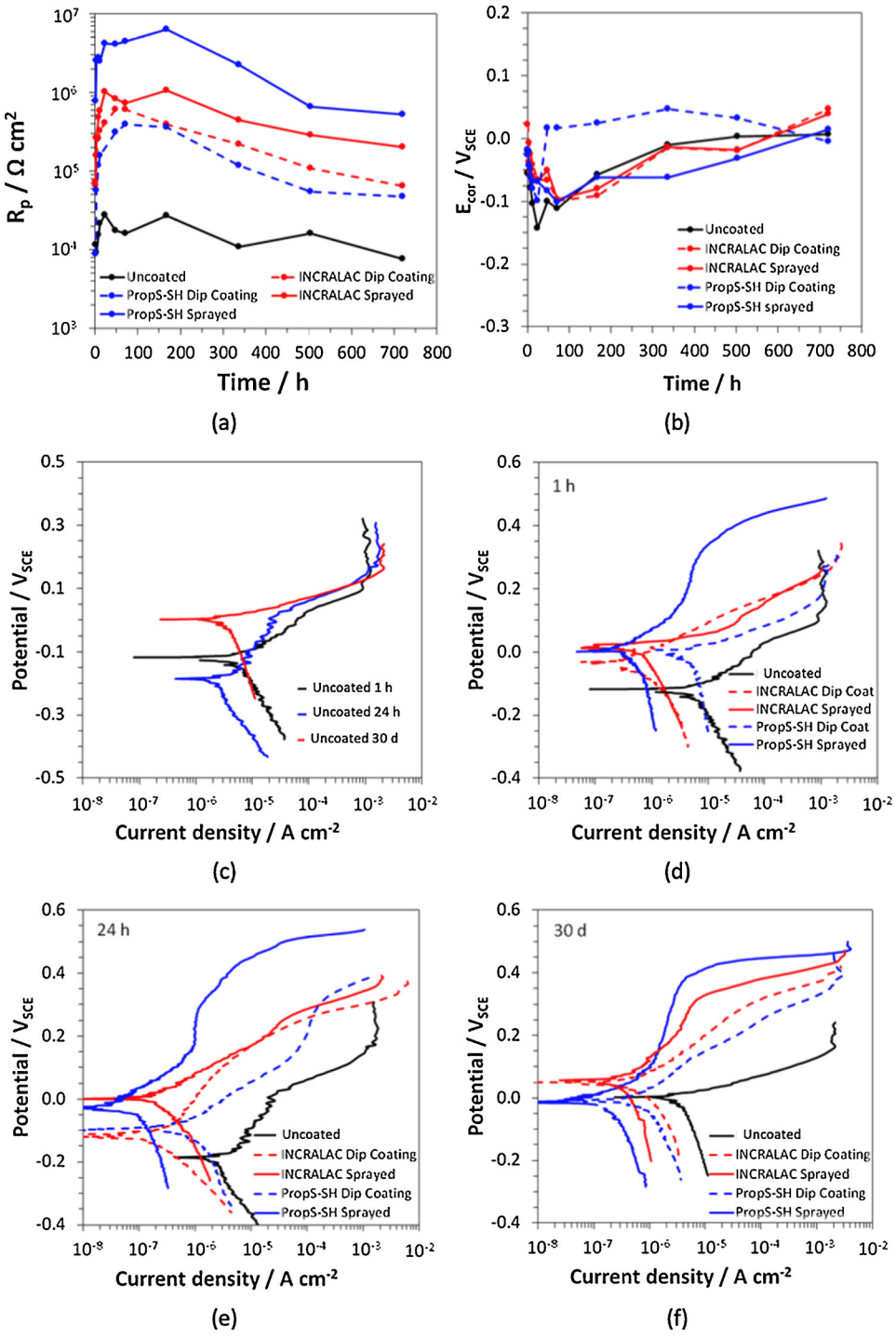

Fig. 3. Electrochemical characterization of uncoated and coated bronzes. Polarization resistance (a) and corrosion potential (b) values recorded during 30 days of exposure to acid rain (ARX10). Polarization curves recorded on uncoated specimens at different immersion times (c) and on uncoated and coated specimens after 1 h (d), 24 h (e) and 30 days (f) of exposure to ARX10. (For interpretation of the references to colour in this figure legend, the reader is referred to the web version of this article).

SEM observations of the uncoated and coated bronze were carried out using a FEG SEM FEI Helios NanoLab 600i coupled to EDS system (Aztec Oxford apparatus, SDD detector, WD 4 mm). After surface ex amination, *in situ* cross sections of specific representative locations were obtained by Focused Ion Beam (FIB) milling (Ga^+ ions) as detailed in [36]. For the surface and cross section imaging, an accelerating voltage of 5 kV and a current intensity of 86 pA was applied, while for the chemical analysis by EDS, 10 kV and 1.4 nA were used. All the samples were carbon coated by sputtering using a Leica ACE 600 for improving conductivity.

X ray Diffraction (XRD) was performed using a SEIFERT XRD 3000 TT diffractometer (Cu Kα, λ = 0.15418 nm). The samples were analysed in grazing incidence mode (GXRD), incident grazing angle of 2°, pattern acquisition from 10° to 80°, 2θ mode, step of 0.03° and step time of 24 s. The analysed surface area corresponds to ~0.5 cm^2.

XPS analyses were carried out using a monochromated Al Kα source (hν = 1486.6 eV) on a ThermoScientific K Alpha system. The X ray spot size was about 400 μm in diameter. The photoelectron emission

Table 1
Corrosion potential (E_{cor}) and current density (J_{cor}) parameters and Protection efficiency (PE) obtained by 30 days polarization curve measurements.

Sample	E_{cor} (V_{SCE})	J_{cor} (μA cm ^{2})	PE (%)
		30 days	
Uncoated bronze	0.003	4.0	–
Incralac® Dip Coating	0.058	0.69	83
Incralac® Sprayed	0.056	0.45	89
PropS-SH Dip Coating	0.015	0.72	82
PropS-SH Sprayed	0.009	0.10	97

spectra were recorded in direct N(Ec). The pass energy was fixed at 130 eV with a step of 1 eV for surveys, and 40 eV with a step of 0.1 eV for core levels. Ionic sputtering of the surfaces was made with Ar^{+} ion beam accelerated under 200 eV at low current for 30 s, in order to re move carbon surface contamination. XPS data were fitted by using Thermo Scientific™ Avantage Software and the Shirley method was used for background subtraction of all the peaks.

3. Results and discussion

3.1. K_2S patina

Macroscale observation of the black patina on CuSi3Mn bronze displays a rather homogeneous surface, black and dark grey in colour (Fig. 2a). The colour coordinates resulting from the average of six samples are: L* = 24 ± 1, a* = 1.3 ± 0.5, b* = 2.1 ± 0.9. SEM ob servation, however, indicates a noticeable surface roughness (Fig. 2b), due to the sandblasting applied before patination. At micrometric scale, the patina surface consists of micrometric grains also enclosing some abrasive particles.

Grazing angle XRD reveals the presence of orthorhombic chalcocite (Cu_2S JCPDS PDF 00 033 0490) and cuprous oxide (Cu_2O JCPDS PDF 01 071 3645), and also confirms the presence of some quartz (SiO_2 JCPDS PDF 01 089 1961) from the sandblasting procedure. A re presentative FIB cross section of the black patina is shown in Fig. 2b. The influence of sand blasting is clearly visible, producing scratches about 10 μm wide and thin cracks in the surface layer of strain har dened bronze. The black patina displays a variable thickness, ranging from 500 nm to about 3 μm. It is characterised by a two layer structure (EDS maps of the FIB cross section in Fig. 2e and f): an internal cuprous oxide layer, covered by an external layer of cuprous sulphide. The in ternal oxide, thin and homogeneous, is due to heating during the pa tination process, before the application of the K_2S solution [37]. The external cuprous sulphide formed mainly small dendritic crystals. GD OES measurements reported in Fig. 2d confirm the FIB observation, showing a thin patina layer (< 1 μm) with an external S rich sub layer and an inner O rich sub layer.

3.2. Preliminary electrochemical evaluation of coating protectiveness

At first, the corrosion behaviour of patinated modern bronze, both uncoated and coated by PropS SH or Incralac®, was monitored by electrochemical tests during exposure to concentrated synthetic acid rain (ARx10). The protection efficiency of the different surface treat ments, applied either by dip coating or by spraying on patinated bronze, as well as of the black patina on the uncoated samples, was firstly investigated by monitoring the time evolution of the polarisation resistance R_p and corrosion potential E_{cor} values. The results obtained during 30 days of continuous exposure to ARX10 are shown in Figs. 3a and 3b.

For the uncoated black patina, the R_p values showed a slight in crease from 11 kΩ cm^2 to 28 kΩ cm^2, during the initial 24 h. Then, despite some fluctuations, they decreased down to 7.9 kΩ cm^2 at the end of the exposure (Fig. 3a), suggesting relatively high degradation rates. The corresponding E_{cor} values evolved from 0.07 V after 1 h immersion to more active values (0.14 V_{SCE}) after 24 h and then con tinuously increased up to 0.007 V_{SCE}, at the end of test (Fig. 3b).

Table 2
Colour variation measurements in CIELab 1976 colour space induced by coating application on black patina on CuSi3Mn.

	Δa*	Δb*	ΔL*	ΔE*
Incralac®	0.5 ± 0.2	1.2 ± 1.4	2.0 ± 1.7	2.9 ± 1.2
PropS-SH	0.2 ± 0.4	1.0 ± 0.4	3.8 ± 0.4	3.8 ± 0.3

During the first week of exposure, PropS SH dip coated bronze specimens exhibited R_p values about one order of magnitude higher than those recorded on the uncoated sample (Fig. 3a). Then, the R_p values tended to decrease slowly, although they always remained much higher than those of the uncoated one(about 47 kΩ cm^2, after 30 days). Even though dip coating produced Incralac® layers with specific weights much higher (5.6 g m^{-2} on average) than those of silane coatings (1.6 g m^{-2} on average), Incralac® led to only slightly higher R_p values, with similar time evolution and final average R_p values of 65 kΩ cm^2 (Fig. 3a). The high initial R_p values suggest that both PropS SH and Incralac® applied by dip coating offer a good protection, involving a good adherence onto the substrate and an effective barrier effect to wards the aggressive environment. However, R_p decreases with time, indicating a slow penetration of the aggressive solution as well as of dissolved oxygen through the coatings, partially impairing their per formances. In order to assess and compare the performance of silane and Incralac®, sprayed coatings of the same specific weight of about 6 g m^{-2} (and hence comparable thickness) were then tested.

Fig. 3a shows that the spraying method led to some improvement in comparison to dip coating. This improvement is much more noticeable in the case of PropS SH, which affords R_p values one order of magnitude higher than those obtained by dip coating, due to its increased thick ness.

The polarization curves recorded at different exposure times on uncoated specimens are collected in Fig. 3c. These curves highlight relatively high initial anodic slopes of about 0.12 V/decade, after 1 h, and 0.24 V/decade, after 24 h of exposure. In this period, the cathodic polarization curve of oxygen reduction tends to shift towards lower current densities. Conversely, at the end of the exposure period (30 days), the anodic slope significantly decreases to about 0.06 V/decade, while the cathodic currents again accelerate. These variations suggest that initially the patina becomes more compact and protective, likely due to the precipitation of insoluble corrosion products, probably cu prous oxide, inside the patina pores. Then, at the end of exposure, prevalent formation of soluble corrosion products appears to occur, because patinated bronze exhibits an active corrosion behaviour, meaning that the patina is not protective anymore.

The polarization curves recorded on PropS SH and Incralac® (de posited by dip coating and by spraying after 1 h, 24 h and 30 days of immersion) are shown in Figs. 3d, 3e and 3f, respectively.

After 1 h exposure (Fig. 3d), all coated bronze specimens showed E_{cor} values nobler than that of uncoated bronze. However, in the case of silane applied by dip coating (1.6 g m^{-2}), a negligible inhibition of the corrosion current density (J_{cor}) was achieved, while the other thicker coatings offered a significant protectiveness. In particular, regardless the application method, Incralac® appreciably inhibited the cathodic process, while PropS SH applied by spraying showed a more significant barrier effect, against both the cathodic and the anodic process. After 24 h of exposure (Fig. 3e), a marked J_{cor} reduction was observed on all coated samples in comparison to their performances at shorter im mersion times, again more evident in the case of sprayed silane. This coating was the most efficient in hindering both the cathodic and the anodic reactions of the corrosion process and afforded J_{cor} values as low

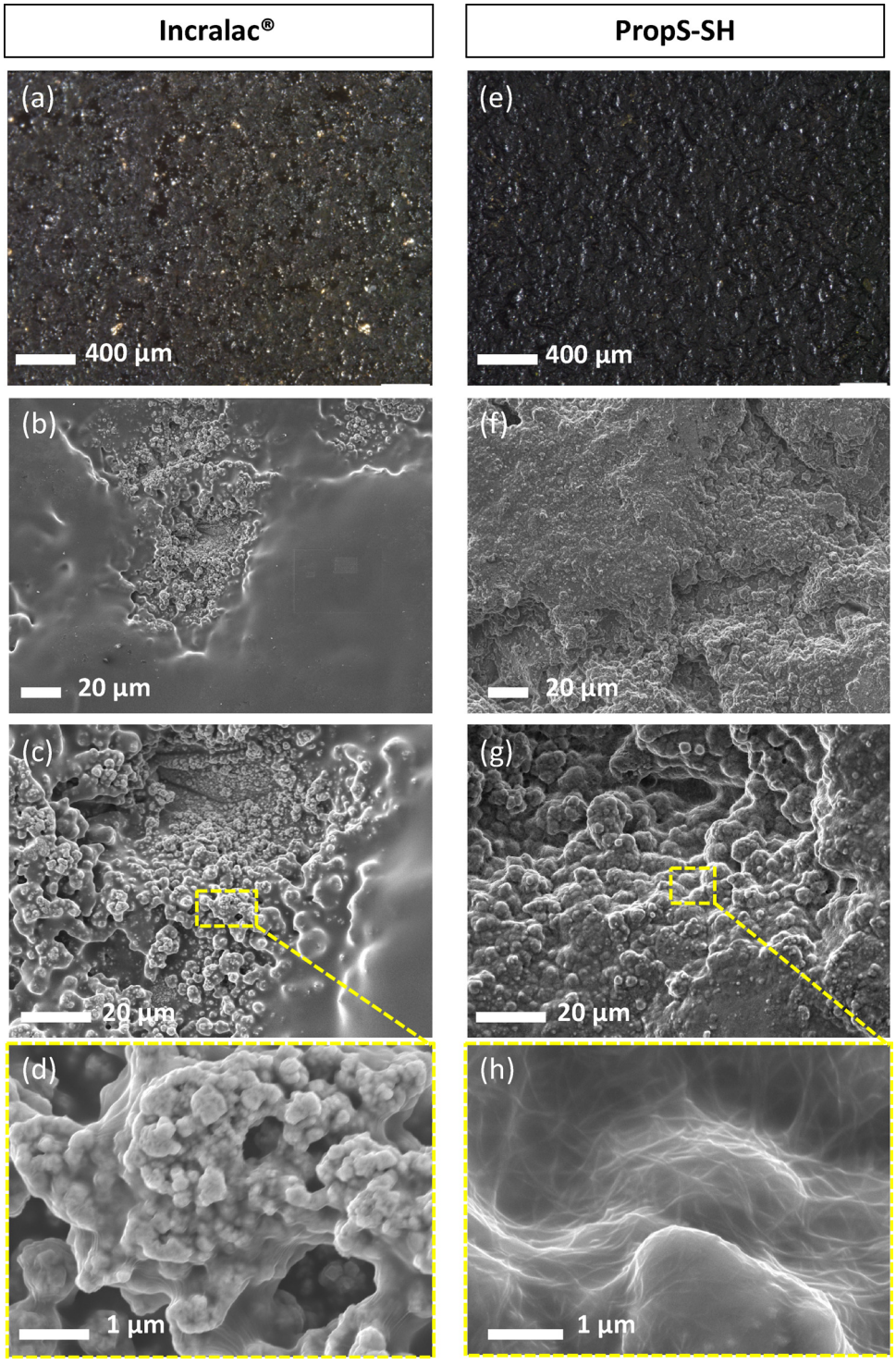

Fig. 4. (a–d) Incralac® and (e–h) PropS-SH surfaces on K_2S-patinated bronze (spraying application of both the coatings), at different magnifications. Optical and SEM observation (SEI).

as $3{\cdot}10^{-8}$ A cm^{-2}. At the end of exposure (Fig. 3f), the corrosion process was slightly accelerated on all specimens, but the sprayed silane still showed a marked reduction of both cathodic and anodic currents in dicating an effective blockage of oxygen reduction process and anodic alloy dissolution. This mixed protective effect was already observed for PropS SH when applied on non patinated copper and bronze as well as on bare magnesium alloys [12,17,19,21,38]. In the case of copper and bronze, FTIR and XPS analyses evidenced that this protective effect was connected to the formation of strong thiolate (Cu−S−C) bonds (from the condensation of SH groups in the silane molecule and Cu−OH groups on copper and bronze surface) [19] and to the development of a rather dense three dimensional Si−O−Si bond network [19,21]. Pore plugging in silane network by insoluble bronze corrosion products contributes to improve the coating barrier effect, as suggested by EIS analysis [12,19].

After 30 days of exposure, high final protective efficiencies (PE) were still calculated by applying Eq. (1), particularly in the case of sprayed PropS SH. Table 1, collecting the E_{cor} and J_{cor} parameters

Table 3
XPS atomic quantification (at%) of Incralac® and PropS-SH coatings before and after dropping test. The XPS measurements were carried out after Ar+ sputtering (200 eV for 30 s).

	C 1 s			N 1 s	O 1 s	Si 2p		S 2p		Cu 2p
	CC, CH, CN, C Si	C-O, C S	C=O O-C=O	N C N O		O Si C Si O Si	SiO_2	C S	Sulphates	Cu(I)
Before ageing										
Incralac®										
Peak BE (eV)	284.7	286.2	288.5	399.6	532.4	101.9	–	–	–	–
at%	61.0	10.4	8.9	0.5	18.6	0.6	–	–	–	–
PropS-SH										
Peak BE (eV)	284.7	286.3	288.2	399.2	532.4	102.4	103.4	163.2	168.1	–
at%	37.4	3.8	0.7	0.3	31.1	14.6	3.2	8.1	0.9	–
After dropping										
Incralac®										
Peak BE (eV)	284.7	286.4	288.5	399.6	532.4	102.3	–	–	–	932.9*
at%	59.0	8.2	11.2	1.1	19.3	1.0	–	–	–	0.3
PropS-SH										
Peak BE (eV)	284.7	286.3	288.2	400.2	532.2	102.1	103.4	163.2	168.1	932.9*
at%	39.4	4.6	3.4	1.4	30.7	8.3	4.6	4.6	2.8	0.2

derived from the 30 days polarization curves, shows that the final PE of sprayed silane is 97%, while those of Incralac® are 83 and 89%, in the case of dip coating or spraying application methods, respectively. The excellent performance of spray coated surfaces is thus confirmed by the electrochemical curve evolution with time.

3.3. Incralac® and PropS SH spray coated surfaces: characterisation before ageing

The influence of silane spraying application on patina colour and contact angle was firstly assessed.

The preliminary optical investigation confirmed the relative homogeneity of all coatings produced by spraying at a macroscale level. As shown in Table 2, both coatings do not induce remarkable colour variations, as the ΔE* values were 2.9 and 3.8 for Incralac® and PropS SH, respectively.

Analogous results were obtained by contact angle measurements on both coatings, showing a contact angle of 81.3° for Incralac® and 80.6° for PropS SH, while for the uncoated bronze the contact angle was 20°.

The morphology of the coated surfaces is displayed in Fig. 4.

Spray application of Incralac® and PropS SH induced the formation of a continuous layer, masking the rough morphology of the black patina previously shown in Fig. 2. However, the surface coated by Incralac® (Fig. 4a d) reveals a very thin coating layer for the areas hardly reachable by the spray jet (bottom of sand blasting grooves). Cu sulphide crystals are still visible, even though partly embedded within the polymeric layer, which also shows some micro porosities (Fig. 4d). Conversely, the PropS SH layer is more homogeneously distributed, as shown in Fig. 4e h. In particular, at higher magnification (Fig. 4h), the silane coating forms a continuous network, efficiently covering the Cu sulphide crystallites of the black patina. This distinction has to be related to the different surface wettability afforded by the two different coating formulations applied. This was confirmed by simple capillary rise measurements performed after partial immersion of the bronze sheets in the coating formulations, followed by sheet drying. The capillary rise after 15 min of partial immersion (2 mm deep) was about 5 mm for Incralac® and 8.5 mm for PropS SH. These results suggested that, for the latter formulation, the attractive forces between solution and black patina overcome the cohesive ones between the solution molecules by a greater extent than in the case of Incralac®. The higher wettability of PropS SH is likely due to the high chemical affinity between the thiol groups and superficial Cu cations [39] in Cu_2S and Cu_2O patina compounds and determines an easier access of the silane solution into surface cavities, due to capillary forces.

The results of XPS analysis of the two coatings applied on black patina are reported in Table 3 and in Fig. 5. They were obtained after a slight Ar^+ etching for limiting C contamination on the top surface. For Incralac®, the top surface mainly consists of C and O with minor contributions from N and Si elements. In particular, C 1 s showed an intense peak centred at BE = 284.6 ± 0.1 eV, characteristic of C C and C H chains of methyl methacrylate and ethyl methacrylate, present in the coating formulation, and two minor peaks at BE = 286.3 ± 0.1 eV and BE = 288.5 ± 0.1 eV, linked to C O and O C = O species, respectively. In addition, O 1 s is mainly linked to C 1 s. This is also confirmed by the atomic quantification reported in Table 3, in which the O element in the coating is completely linked to C, with a C/O atomic ratio of about 1. N was detected in low concentration (N 1 s, BE = 399.5 ± 0.1 eV), highlighting the presence of BTA corrosion inhibitor within the organic layer, as reported in [40 42].

Regarding the top surface of PropS SH, the main elements detected are C, O, Si and S, as expected. In particular, C 1 s showed an intense peak at BE = 284.6 ± 0.1 eV, characteristic of the aliphatic chain of the coating and also two other small contributions (BE = 286.3 ± 0.1 eV and BE = 288.2 eV) linked to C–S/C–O and O–C=O species, respectively. An intense Si 2p peak was observed at BE = 102.3 ± 0.1 eV, ascribed to the silane (C–Si–O and Si–O–Si), as detailed in [13,43]. A small concentration of SiO_2 (BE = 103.4 ± 0.1 eV) was also found. The analysis of S 2p signal takes into account the presence of a doublet structure of the core level with a spacing of 1.2 eV (S $2p_{1/2}$ S $2p_{3/2}$ = 1.2 eV) and a theoretical intensity ratio of 2 (I(S $2p_{3/2}$) / I(S $2p_{1/2}$) = 2). In particular, S 2p peak is centred at BE = 163.3 ± 0.1 eV, characteristic of S–C bonds and thiol groups. It also shows a minor contribution centred at BE = 168.1 ± 0.1 eV, to be ascribed to the presence of sulphate groups [13,43 46], as highlighted in Fig. 5 (dashed line). O–C=O and sulphate bonds are connected to a limited oxidation of the coating, as already observed for organic thiol compounds, such as PropS SH, exposed to the atmosphere [14,47 49]. It is unclear if also the small concentration of SiO_2 (peak at BE = 103.4 ± 0.1 eV) could be related to silane oxidation or to contamination of the original silane monomer commercial product. From the atomic quantification reported in Table 3, the atomic ratios were calculated by considering only the concentration of Si 2p corresponding to the BE value related to silane (BE = 102.4 eV). The obtained values (Si/C = 0.35, Si/O = 0.47 and Si/S = 1.60) are in rather good agreement with the theoretical ones (Si/C = 0.33, Si/O = 0.67 and Si/S = 1.00), indicating that the Ar^+ ion sputtering is efficient in removing contamination without damaging the polymer. However, the Si/O and Si/S ratios are respectively slightly lower and higher than the theoretical ones. The former difference is linked to the additional contribution of SiO_2 species found on this coated substrate, while the latter one is likely due to a loss of sulphur from the silane top layer after thiol group oxidation to volatile sulphur oxide [49].

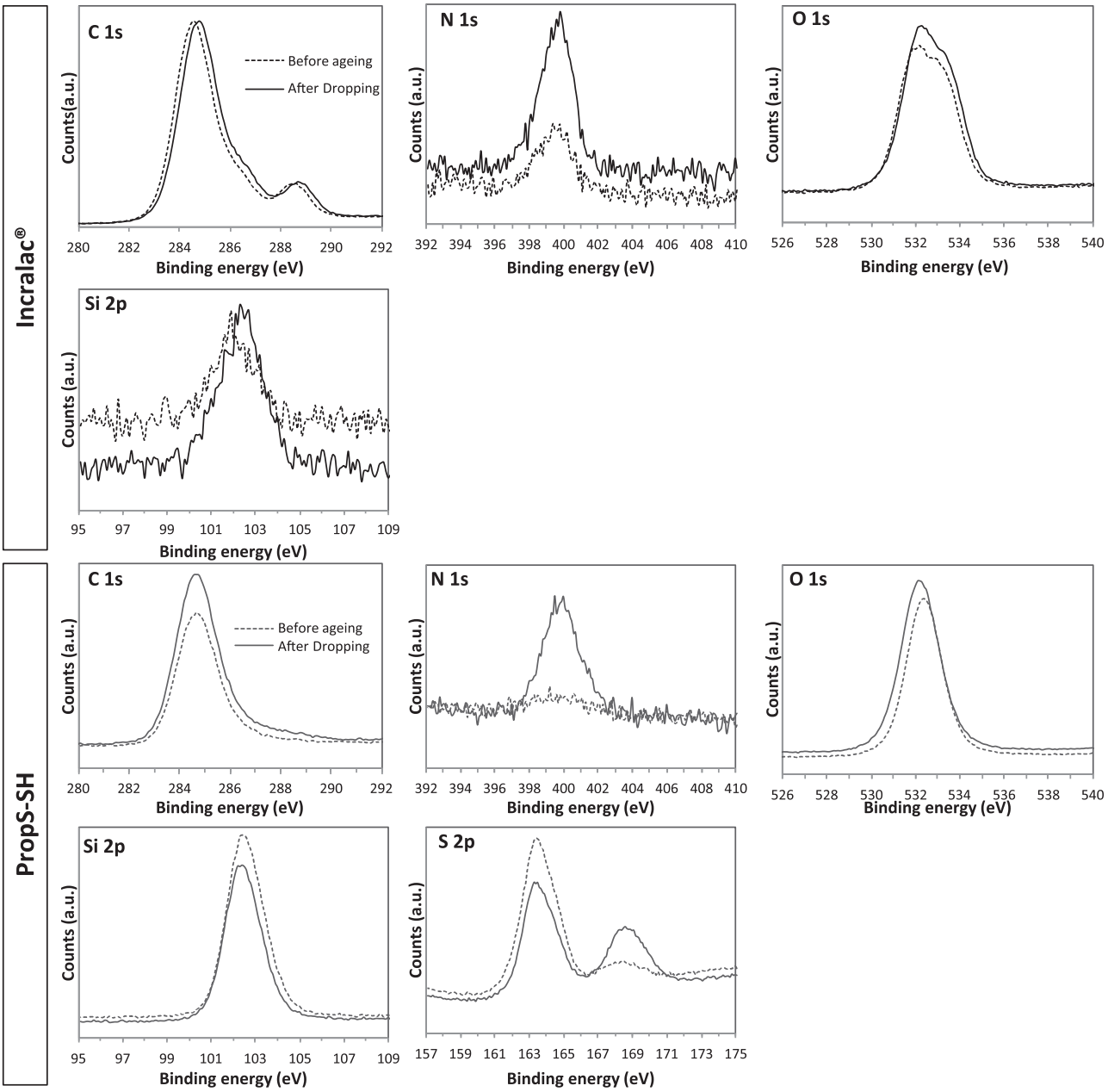

Fig. 5. XPS core levels of the characteristic elements of Incralac® and PropS-SH surface before (dashed line) and after ageing (solid line) by dropping.

3.4. Evaluation of the coatings protectiveness by accelerated ageing

3.4.1. Colour variation after UV/temperature exposure

A first assessment of the protectiveness of PropS SH coating, prepared by spray application, was performed after the exposure to UV and temperature cycles. PropS SH coating underwent a negligible colour variation. In particular, the following variations were calculated: $\Delta a^* = 0.1 \pm 0.1$, $\Delta b^* = 0.1 \pm 0.3$ and $\Delta L^* = -0.9 \pm 0.2$. Therefore, the total colour variations of PropS SH coating after UV cycles could be considered as non noticeable, indicating that, in the presence of the commercial UV stabilizer, PropS SH performs well under the synergistic exposure to temperature changes (ranging from 0 °C to 35 °C) and UV radiation.

3.4.2. Surface evolution during dropping test and inhibiting efficiency

The evolution of uncoated and coated samples exposed to accelerated ageing by dropping test was monitored within a total Time of Wetness (ToW) of 10 days. Mass variations recorded during the test as a function of ToW are reported in Fig. 6. These results confirm the protective barrier effect of both coatings obtained by spray application. Thus, while uncoated bronze exhibits a marked linear trend ($R^2 = 0.997$) of mass decrease with ToW, the coated samples only reveal a very limited mass decrease. However, at the end of ageing, a slight weight increase was measured for Incralac®. This can be due to localised corrosion at the coating/substrate interface, as detailed later, locally inducing corrosion deposits. Possible water absorption by the coating is considered less likely as the weight increase is recorded only at the end of the ageing.

The evolution with ToW of Cu, Mn and Si release in the weathering solutions is shown in Fig. 7. Regarding Si, for both PropS SH and Incralac® coated samples, its concentration in solution was always under the Limit of Detection (LoD = 18 μg L^{-1}), therefore Si release was reported in Fig. 7 only for uncoated samples and η_{Si} was not calculated.

Linear release trends were detected for Cu, Mn and Si. In the case of uncoated samples, Cu/Mn and Cu/Si weight concentration ratios (about 36 and 6, respectively) are much lower than in the alloy (about 96 and

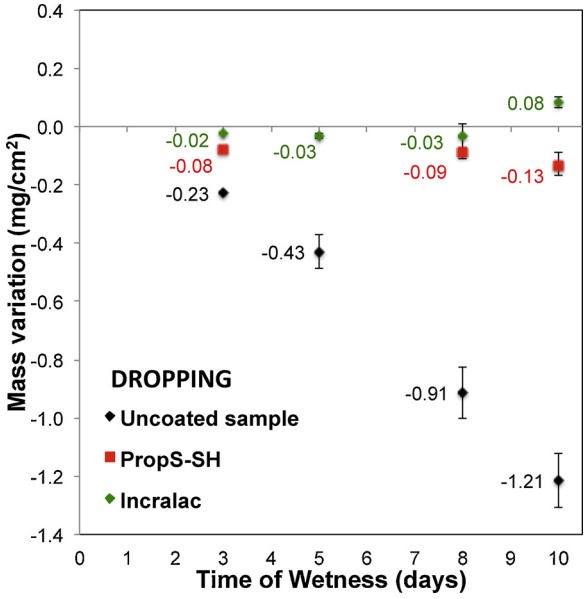

Fig. 6. Mass variation for the uncoated (black dataset) and coated bronze samples (PropS-SH and Incralac® by spraying in red and in green, respectively) during accelerated ageing by dropping test (For interpretation of the references to colour in this figure legend, the reader is referred to the web version of this article).

31), likely due to a preferential dissolution of Mn and Si alloying elements in the weathering solutions, while Cu species precipitate on the surface forming a porous Cu oxide deposit, as detailed hereafter. This result highlights that the dropping test always leads to a significant surface leaching for uncoated bronze, thus preventing the formation of a protective barrier layer of Cu based corrosion products.

By comparison to the uncoated ones, the coated samples displayed a much lower dissolution rate for all the analysed metallic elements without marked surface modification (as detailed later), clearly confirming the high protectiveness of both coatings. Inhibiting efficiency values (η), calculated by Eq. (3), quantify these differences. In particular, Incralac® afforded average η_{Cu} values of 92 and η_{Mn} of 95, while PropS SH showed η_{Cu} of 95 and η_{Mn} of 87, confirming an excellent and comparable protective performance of these coatings.

3.4.3. *Surface characterisation after accelerated ageing by dropping*

After dropping, the uncoated patinated Cu Si Mn bronze underwent extensive degradation due to corrosion, compared to the coated ones that did not exhibit corrosion (Fig. 8). These results from surface morphology observation were in agreement with gravimetric and metal release data, discussed in Section 3.4.2.

On the uncoated samples (Fig. 8a), the formation of Cu based corrosion products, linked to a significant evolution of the black patina, was observed. Due to runoff and high Cu ions release in the ageing solution, the initial rough surface was still observable, but it was partially masked by the formation of a new layer of cubic crystallites (Fig. 8b). XRD measurements revealed that these Cu species consist of cuprous oxide (Cu_2O JCPDS PDF 01 071 3645), but they also indicate the presence of orthorhombic Cu_2S (JCPDS PDF 00 033 0490) and residual quartz particles due to sandblasting (JCPDS PDF 01 089 1961). No hydroxysulphate salts were identified. The samples coated by PropS SH

(Figs. 8 e and f) did not show remarkable differences by comparison to the surfaces before ageing (Fig. 4). However, the Incralac® coating exhibits a smoother surface, characterised by cracks after dropping

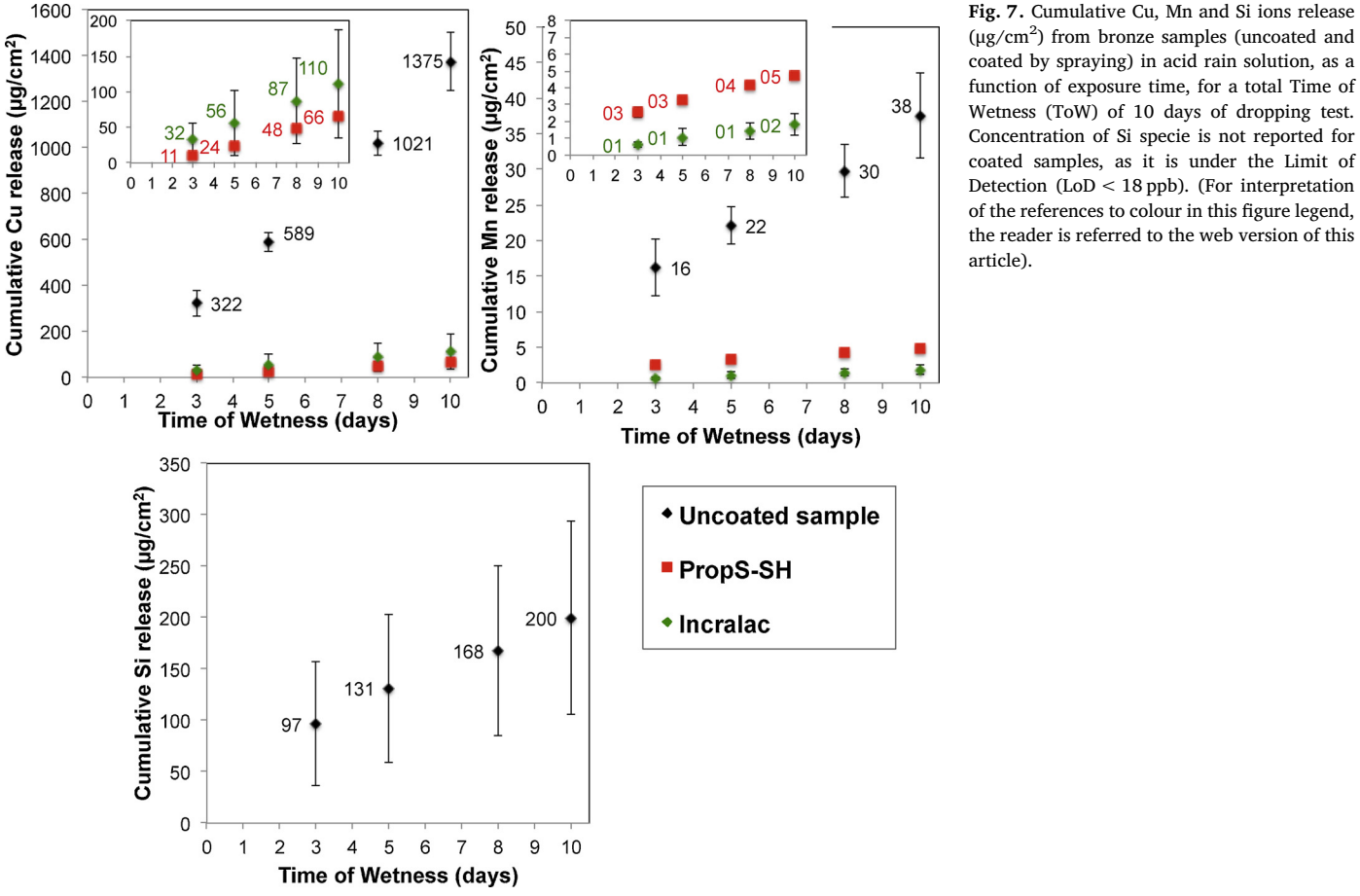

Fig. 7. Cumulative Cu, Mn and Si ions release (µg/cm²) from bronze samples (uncoated and coated by spraying) in acid rain solution, as a function of exposure time, for a total Time of Wetness (ToW) of 10 days of dropping test. Concentration of Si specie is not reported for coated samples, as it is under the Limit of Detection (LoD < 18 ppb). (For interpretation of the references to colour in this figure legend, the reader is referred to the web version of this article).

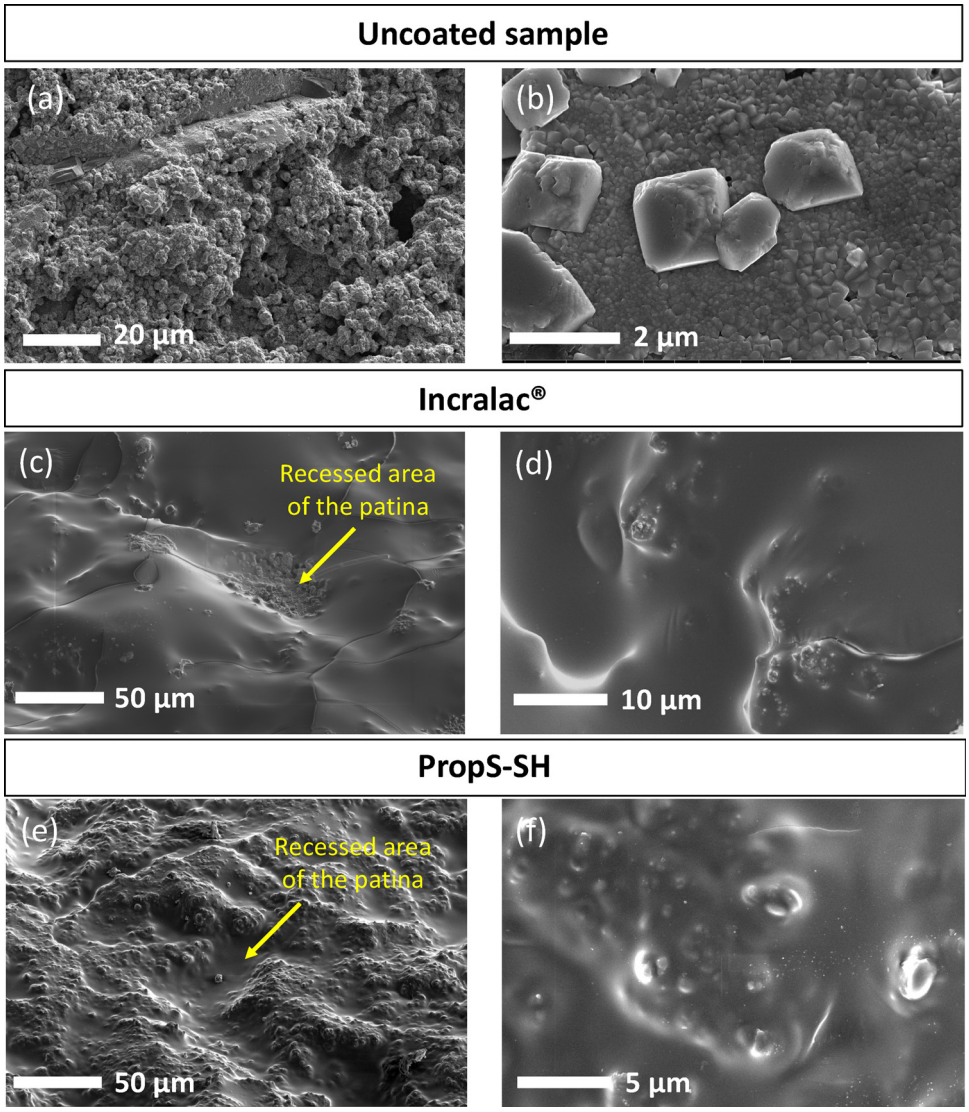

Fig. 8. Surface morphology after dropping: (a, b) Uncoated bronze; (c, d) bronze coated by Incralac® (e, f); bronze coated by PropS-SH (both the coatings were applied by spraying).

Table 4
Colour variation measurements in CIELab 1976 colour space induced by accelerated ageing (dropping test).

	Δa*	Δb*	ΔL*	ΔE*
Uncoated sample	0.9 ± 0.7	4.1 ± 2.2	7.5 ± 1.6	8.8 ± 1.6
Incralac®	0.3 ± 0.5	0.8 ± 1.0	0.4 ± 1.1	1.2 ± 1.2
PropS-SH	0.4 ± 0.2	0.20 ± 0.03	0.5 ± 0.3	0.7 ± 0.2

(Fig. 8c and d), which were not observed for PropS SH (Fig. 8e and f). Furthermore, surface alterations appeared in areas exhibiting lower thickness of the protective coatings. For Incralac®, this occurs in correspondence with recessed areas (*e.g.* bottom of sand blasting grooves Fig. 8c) while for PropS SH (*i.e.* for the surface treatment with higher penetration capability), this occurs on raised areas (*i.e.* upper part of grooves Fig. 8e).

In addition, colour measurements reported in Table 4 revealed that the uncoated bronze undergoes marked colour change during dropping ($\Delta E^* \sim 9$). This change was mainly due to an increase in lightness ($\Delta L^* \sim 7.5$) and to chromatic variations towards blue. On the contrary, the colour of coated samples did not significantly change due to dropping test ($\Delta E^* < 3$). No evident alteration of the aesthetical appearance was detected, especially for PropS SH coated surfaces, indicating a good protectiveness without patina evolution and formation of corrosion products.

The influence of dropping on the two coatings was analysed also by XPS measurements. Results are reported in Fig. 5, comparing the reported core levels before (dashed line) and after (solid line) the dropping test. Atomic quantification measured on their top surfaces after ageing is reported in Table 3. For Incralac®, the results show that no significant variation occurred, except a slight increase in N 1 s and Si 2p. In parallel, on the top surface of PropS SH, no strong differences in the environment of the main elements (C 1 s, O 1 s, Si 2p, S 2p and Cu 2p) was observed, as shown in Fig. 5. This confirms that no marked modification of the coating surface chemistry occurred after ageing. In addition, as detailed in Table 3, dropping induced an increase in N 1 s contribution. This could be ascribed to the presence of nitrate species from the acid rain solution on the outermost coating layers. An increase of SO_x species at BE = 168.1 ± 0.1 eV for S 2p was also detected. This increase is related to oxidation of silane coatings and to the presence of sulphates among the corrosion products, as observed in a previous study [49]. However, even if Cu 2p signal slightly increased after dropping, Cu remained present in very low concentration with a not well resolved Cu 2p signal.

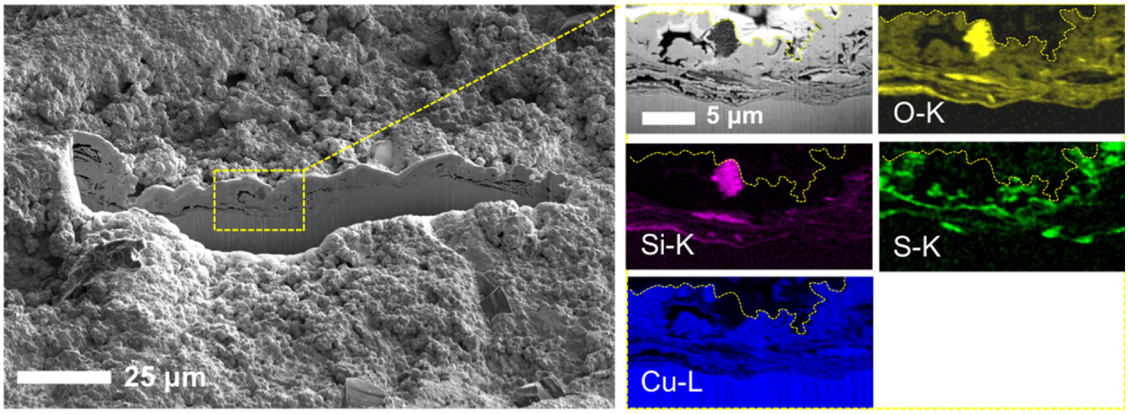

Fig. 9. FIB cross-section of the uncoated bronze after dropping. X-ray maps of both the cross-sections show the distribution of O, Si, S and Cu (Mn is not reported as the EDS map is not well-resolved). Pt-C layer was applied before FIB milling in order to protect the top surface of the cross-section. (For interpretation of the references to colour in this figure legend, the reader is referred to the web version of this article).

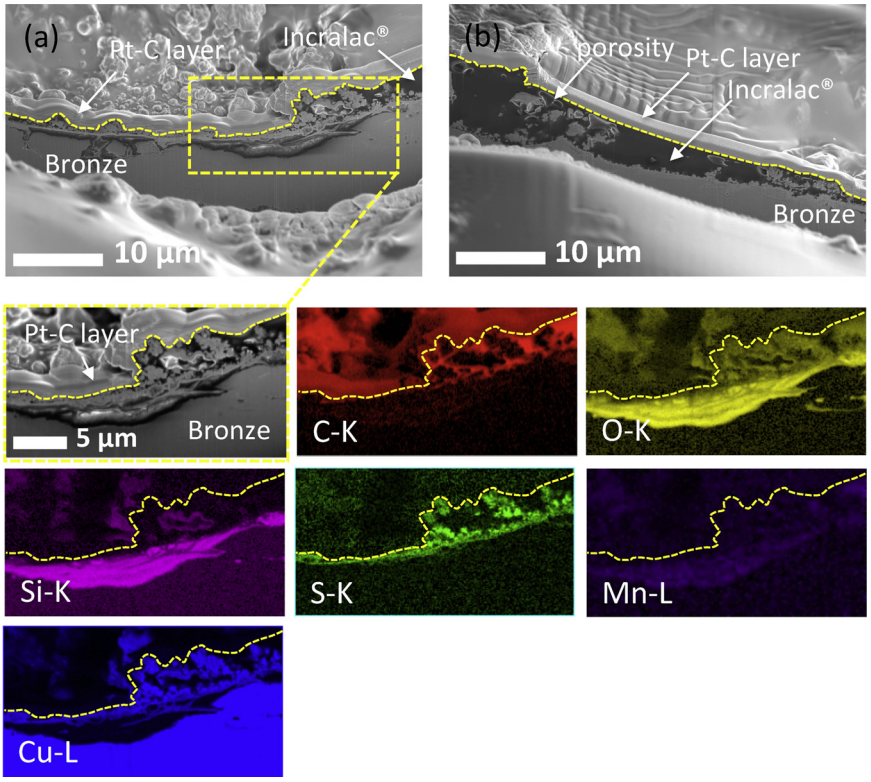

Fig. 10. FIB cross-section of the bronze coated by Incralac® (applied by spraying) after ageing by dropping, in correspondence of (a) a thinner part (recessed parts) and (b) coating thicker part, corresponding to raised areas of the bronze, i.e. on the top of grooves induced by sand-blasting). X-ray maps on cross-section revealing the distribution of the main elements in the coated system (area outlined by the dashed yellow line in (a)). Pt-C layer was applied before FIB milling in order to protect the top surface of the cross-section (For interpretation of the references to colour in this figure legend, the reader is referred to the web version of this article).

3.4.4. Cross section examination after accelerated ageing by dropping

Investigation of the microstructure of the coating/patina/bronze system after ageing was performed by FEG SEM observation of *in situ* FIB cross sections. The results for uncoated samples are shown in Fig. 9. By comparison with the examination before ageing reported in Fig. 2, the corrosion process induced a marked modification of the patina structure. Internal preferential dissolution of Cu is observed, producing numerous voids and exfoliations within the corrosion modified patina. This is accompanied by a relative enrichment in Si and O, forming an internal corrosion layer in which S element is also observed.

Therefore, a decuprification process may take place, characterized by the internal oxidation of the alloy with preferential dissolution of Cu ions and a relative enrichment in oxidised Si. This phenomenon appears similar to the corrosion behaviour highlighted for tin bronze [16]. In that case, selective dissolution of Cu, due to internal oxidation, induces selective enrichment in the stable oxidised Sn alloying element. However, in the case of the Cu Si Mn bronze, further work is needed to study the corrosion behaviour in more detail.

As regards the coated samples, FIB cross section observations are reported in Figs. 10 and 11 for Incralac® and PropS SH, respectively. In general, the coatings fully cover the black patina, filling up the porosities among black Cu sulphide crystallites. This microstructural characterisation confirms the surface observations performed before ageing. For both coatings, the polymer layer is not homogenous in thickness. Its thickness ranges from about 150 nm (Figs. 10 and 11b) to several micrometres: about 10 µm for Incralac® and 7 µm for PropS SH (Figs. 10b and 11a respectively). However, as previously pointed out (Fig. 4), the thickness variations of Incralac® are opposed to those of PropS SH, due to the fact that PropS SH exhibited higher wettability compared to Incralac® on the black patina, as previously discussed. In fact, Incralac® is thicker on the raised areas of the patinated bronze (*i.e.* on the top areas of sand blasting grooves) and very thin in the lower recessed parts. The opposite occurs for PropS SH film.

Fig. 10 also shows that large pores are visible inside the Incralac®

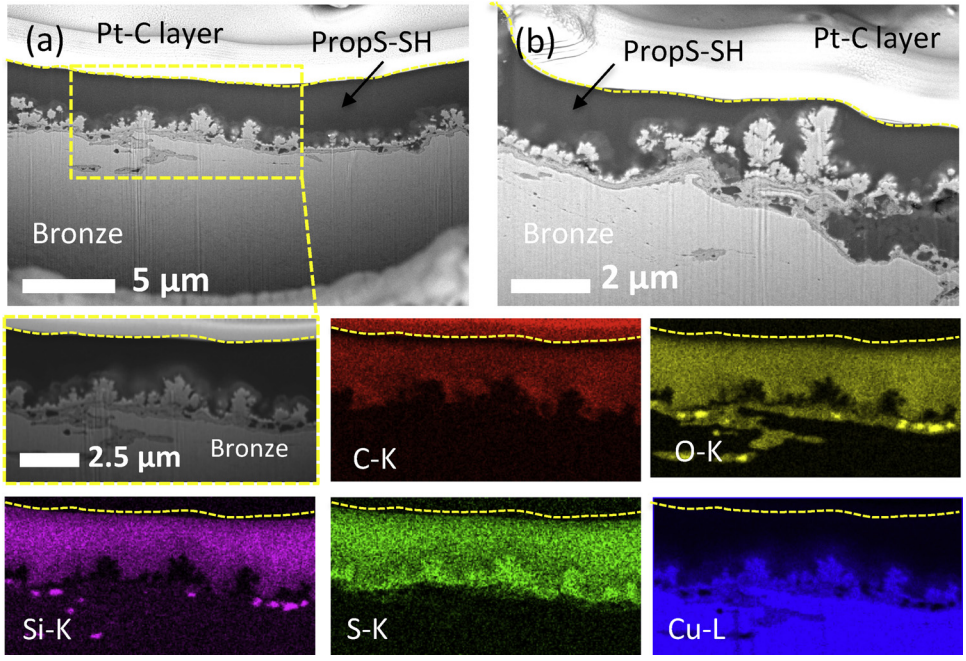

Fig. 11. FIB cross-section of the bronze coated by PropS-SH (applied by spraying) after ageing by dropping, in correspondence of (a) thick part located in the recessed parts and (b) thin part (raised area of the bronze surface) of the bronze surface. X-ray maps on cross-section of the main elements located within the coated system after ageing. Pt-C layer was applied before FIB milling in order to protect the top surface of the cross-section.

layer, with diameters ranging from 1 to several µm, sometimes in contact with the black patina. Conversely, PropS SH (Fig. 11) is dense and well adherent to the underlying black patina.

Such differences are connected to a different wettability of the black patina by the coating formulations. In fact, the high affinity of the thiol groups with the Cu cations of the patina is expected to particularly favour the penetration of hydrolized PropS SH solution inside the pa tina pores and cavities, by the contribution of capillary forces. This property of the PropS SH solution can improve the adherence of the obtained coating onto the patina and increase its protectiveness against bronze corrosion, even if the contributions of other factors, such as density of the polymeric network, pore dimensions, pore plugging capability by corrosion products cannot be excluded and are worthy of further investigations.

Because of the observed thickness variations in the studied coatings, corrosion started within the thinnest part of the coatings, inducing possible localised corrosion attacks which could be on the recessed areas for Incralac® and on raised areas for PropS SH.

For Incralac®, this is shown in Fig. 10a (SEM image), and by the corresponding X ray maps of C and O elements (polymeric coating) as well as of Si, Cu and Mn (patina). Corrosion, developed at the bronze/ black patina interface, produces Cu based corrosion products (Cu and O elements on the coating surface) and an internal corrosion layer under the initial patina. This is highlighted by the presence of large amounts of oxygen under the sulphide layer (Fig. 10). The X ray map of O ele ment, together with those of S and Cu, clearly shows that, as for the uncoated sample (Fig. 9), a decuprification process occurred, char acterised by a marked Cu dissolution (low Cu signal) and a relative enrichment in Si (high Si signal) as well as in Mn, even though to a lower extent (the x ray map of Mn was not reported in Fig. 9 because of its low resolution, however the comparison of localised EDS micro analysis data pointed out this phenomenon).

For PropS SH coating after dropping, the FIB cross section did not reveal a clear corrosion attack at the coating substrate interface (Fig. 11), as demonstrated also by x ray maps in Fig. 11. The original structure of the initial black patina (previously reported in Fig. 2) is apparently conserved, indicating that also a thin layer of PropS SH is able to protect the substrate from corrosion.

These findings suggest that, even if the two coatings exhibit very low and comparable metal releases from the substrate, in terms of η_{Cu} and η_{Mn} values (section 3.4.2), only PropS SH efficiently prevents alloy corrosion. Instead, Incralac® cannot avoid the formation of Si and Mn enriched layers under the patina (EDS x ray maps in Fig. 10), related to localised corrosion in thinner areas of the coating according to its lower wettability.

4. Conclusions

The assessment of the protectiveness of 3 mercapto propyl tri methoxysilane (PropS SH) coating applied on K_2S patinated CuSi3Mn bronze was carried out. The following main conclusions can be drawn from this work:

- The K_2S patina applied by torch technique on silicon bronze forms a double layer structure: an internal cuprous oxide layer, directly re lated to surface heating during the patination process, covered by an external one mainly consisting of cuprous sulphide (small coalesced crystals), identified by XRD and *in situ* FIB cross section.
- Based on results from electrochemical tests, thicker PropS SH and Incralac® coatings applied by spraying offer a good protection to patinated bronze, better than by dip coating, particularly in the case of PropS SH. Protective efficiency (PE) values of sprayed coatings are 97 and 89% for silane and Incralac®, respectively.
- Incralac® and PropS SH coatings applied by spraying produce con tinuous layers. However, Incralac® does not completely penetrate within patina cavities, whereas PropS SH is found to cover more homogenously the patinated surface due to its higher wettability.
- Black patina on Cu Si Mn bronze, if not protected, undergoes colour and morphological change. PropS SH (with a commercial UV sta bilizer) coatings show excellent performance under UV/temperature cycles in terms of colour variation, being the total colour change non noticeable ($\Delta E^* = 1.0 \pm 0.1$).
- Accelerated ageing by dropping does not induce strong variation in the chemistry of both coating layers, indicating a good stability of the polymer/patina system. A slightly higher inhibiting efficiency in terms of metal release (η_M) was measured for PropS SH. In fact, based on cross section examination, PropS SH seems to better pre vent the accumulation of insoluble corrosion products, compared to Incralac®, which cannot avoid the formation of a Si enriched cor rosion layer in the thinner coating zones, suggesting the onset of

decuprification when exposed to acid rain.

Acknowledgements

This work has been performed in the scope of the B IMPACT project within the M ERA.NET network, supported by national funding orga nisations (MIZŠ Slovenia, MIUR Italy, RMP France).

The authors wish to thank: Livartis d.o.o. (Slovenia) for producing quaternary alloy bronzes (www.livartis.si/en) and Dr. Cédric Charvillat (CIRIMAT, University of Toulouse) for XRD measurements. Dr. Iuri Boromei (Dept. of Industrial Engineering at the University of Bologna) is gratefully acknowledged for GD OES analyses of the K_2S patinated bronze.

References

[1] V. Alunno Rossetti, M. Marabelli, Analyses of the patinas of a gilded horse of St Mark's Basilica in Venice: corrosion mechanisms and conservation problems, Estud. Conserv. E Restauro 21 (1976) 161–170.
[2] J. Wolfe, R. Grayburn, A review of the development and testing of Incralac lacquer A review of the development and testing of Incralac lacquer, J. Am. Inst. Conserv. (2017) 1–20, https://doi.org/10.1080/01971360.2017.1362863.
[3] http://www.conservationsupportsystems.com/product/show/incralac-solvent-based/metal-coatings, (n.d.).
[4] J. Kim, K. Chang, T. Isobe, S. Tanabe, Acute toxicity of benzotriazole ultraviolet stabilizers on freshwater crustacean (Daphnia pulex), J. Toxicol. Sci. 36 (2011) 247–251.
[5] G. Bierwagen, T.J. Shedlosky, K. Stanek, Developing and testing a new generation of protective coatings for outdoor bronze sculpture, Prog. Org. Coat. 48 (2003) 289–296, https://doi.org/10.1016/j.porgcoat.2003.07.004.
[6] M. Pilz, H. Romich, Sol-gel derived coatings for outdoor bronze conservation, J. Sol-gel Sci. Technol. 8 (1997) 1071–1075.
[7] E. Bescher, J.D. Mackenzie, Sol-gel coatings for the protection of brass and bronze, J. Solgel Sci. Technol. 26 (2003) 1223–1226, https://doi.org/10.1023/A:1020724605851.
[8] A. Colledan, A. Frignani, V. Grassi, F. Zucchi, Inhibiting treatments for outdoor bronzes, Proc. 10th Eur. Symp. Corros. Scale Inhib. (10 SEIC), (2005) pp. 843–858.
[9] L.B. Brostoff, E. De La Rie, Research into protective coating systems for outdoor bronze sculpture and ornamentation, Conférence Int. Sur La Conserv. Des Métaux, (1997), pp. 242–244.
[10] H. Fan, S. Li, Z. Zhao, H. Wang, Z. Shi, L. Zhang, Inhibition of brass corrosion in sodium chloride solutions by self-assembled silane films, Corros. Sci. 53 (2011) 4273–4281, https://doi.org/10.1016/j.corsci.2011.08.039.
[11] M. Kozelj, A.S. Vuk, I. Jerman, B. Orel, Corrosion protection of Sunselect, a spectrally selective solar absorber coating, by (3-mercaptopropyl)trimethoxysilane, Sol. Energy Mater. Sol. Cells 93 (2009) 1733–1742, https://doi.org/10.1016/j.solmat.2009.05.023.
[12] F. Zucchi, V. Grassi, A. Frignani, G. Trabanelli, Inhibition of copper corrosion by silane coatings, Corros. Sci. 46 (2004) 2853–2865, https://doi.org/10.1016/j.corsci.2004.03.019.
[13] Y.S. Li, W. Lu, Y. Wang, T. Tran, Studies of (3-mercaptopropyl)trimethoxylsilane and bis(trimethoxysilyl)ethane sol-gel coating on copper and aluminum, Spectrochim. Acta - Part A Mol. Biomol. Spectrosc. 73 (2009) 922–928, https://doi.org/10.1016/j.saa.2009.04.016.
[14] C. Chiavari, A. Balbo, E. Bernardi, C. Martini, F. Zanotto, I. Vassura, et al., Organosilane coatings applied on bronze: influence of UV radiation and thermal cycles on the protectiveness, Prog. Org. Coat. 82 (2015) 91–100, https://doi.org/10.1016/j.porgcoat.2015.01.017.
[15] A. Balbo, A. Frignani, C. Monticelli, Influence of nanoparticles on the inhibiting efficiency of organosilane coatings on bronze. Part 1: electrochemical characterization, Eurocorr 2012 (EFC Event n.330), EFC, London, UK (CD-ROM) (2012) 1–8 Paper 1524.
[16] E. Bernardi, C. Chiavari, B. Lenza, C. Martini, L. Morselli, F. Ospitali, et al., The atmospheric corrosion of quaternary bronzes: the leaching action of acid rain, Corros. Sci. 51 (2009) 159–170, https://doi.org/10.1016/j.corsci.2008.10.008.
[17] C. Chiavari, A. Balbo, E. Bernardi, C. Martini, M.C. Bignozzi, M. Abbottoni, et al., Protective silane treatment for patinated bronze exposed to simulated natural environments, Mater. Chem. Phys. 141 (2013) 502–511, https://doi.org/10.1016/j.matchemphys.2013.05.050.
[18] W.J. van Ooij, D. Zhu, M. Stacy, A. Seth, T. Mugada, J. Gandhi, et al., Corrosion protection properties of organofunctional silanes—an overview, tsinghua sci, Technol. 10 (2005) 639–664, https://doi.org/10.1016/S1007-0214(05)70134-6.
[19] F. Zucchi, A. Frignani, V. Grassi, G. Trabanelli, M. Dal Colle, The formation of a protective layer of 3-mercapto-propyl-trimethoxy-silane on copper, Corros. Sci. 49 (2007) 1570–1583, https://doi.org/10.1016/j.corsci.2006.08.019.
[20] E. Joseph, P. Letardi, R. Mazzeo, S. Prati, M. Vandini, Innovative treatments for the protection of outdoor bronze monuments, Met. 2007 (2007) 71–77.
[21] A. Balbo, C. Chiavari, C. Martini, C. Monticelli, Effectiveness of corrosion inhibitor films for the conservation of bronzes and gilded bronzes, Corros. Sci. 59 (2012) 204–212, https://doi.org/10.1016/j.corsci.2012.03.003.
[22] C. Chiavari, E. Bernardi, C. Martini, F. Passarini, F. Ospitali, L. Robbiola, The atmospheric corrosion of quaternary bronzes: the action of stagnant rain water, Corros. Sci. 52 (2010) 3002–3010, https://doi.org/10.1016/j.corsci.2010.05.013.
[23] C. Chiavari, E. Bernardi, A. Balbo, C. Monticelli, S. Raffo, M.C. Bignozzi, et al., Atmospheric corrosion of fire-gilded bronze: corrosion and corrosion protection during accelerated ageing tests, Corros. Sci. 100 (2015) 435–447, https://doi.org/10.1016/j.corsci.2015.080.013.
[24] Casting of copper and copper alloys casting, ASM Handbook vol 15, ASM Int., 2008, pp. 1026–1048.
[25] P.D. Weil, A review of the history and practice of patination, Corros. Met. Artifacts a dialogue between conserv, Archaeol. Corros. Sci. 479 (1977) 77.
[26] I.Z. Balta, L. Robbiola, Study of black patinas on copper and bronze obtained by using 19th century western traditional techniques of artificial patination, Proc.8th Int. Conf. Non-Destructive Investig. Microanal. Diagnostics Conserv. Cult. Environ. Herit. (2005).
[27] I.Z. Balta, L. Robbiola, Characterization of artificial black patinas on artistic cast bronze and pure copper by using SEM–EDS and light microscopy, Proc. 13th Eur. Microsc. Congr. 22–27 August 2004, Antwerp, Belgium, EMC 2004 CD-Rom Conf. Prepr. (2004).
[28] E. Bernardi, C. Chiavari, C. Martini, L. Morselli, The atmospheric corrosion of quaternary bronzes: an evaluation of the dissolution rate of the alloying elements, Appl. Phys. A Mater. Sci. Process. 92 (2008) 83–89, https://doi.org/10.1007/s00339-008-4451-0.
[29] L. Robbiola, C. Fiaud, S. Pennec, New model of outdoor bronze corrosion and its implications for conservation, ICOM Comm. Conserv. Tenth Trienn. Meet. (1993) 796–802. August 199.
[30] A. Cohen, Properties of cast copper alloys, properties and selection: nonferrous alloys and special-purpose materials, ASM Handbook vol 2, ASM Int., 1990, pp. 356–391.
[31] R. Hughes, Artificial Patination, Butterworth-Heinemann Oxford, 1993.
[32] G. Masi, C. Chiavari, J. Avila, J. Esvan, S. Raffo, M.C. Bignozzi, et al., Corrosion investigation of fire-gilded bronze involving high surface resolution spectroscopic imaging, Appl. Surf. Sci. 366 (2016) 317–327, https://doi.org/10.1016/j.apsusc.2016.01.101.
[33] C. Chiavari, E. Bernardi, C. Martini, L. Morselli, F. Ospitali, L. Robbiola, et al., Predicting the corrosion behaviour of outdoor bronzes: assessment of artificially exposed and real outdoor samples, Met. 2010, Proc. Interim Meet. ICOM-CC Met. Work. Group, Oct. 11-15, 2010 (2011) 218–226.
[34] W.S. Mokrzycki, M. Tatol, Colour differenceΔ E-A survey, Mach. Graph. Vis. 8 (2012).
[35] C. Chiavari, E. Bernardi, D. Cauzzi, S. Volta, M.C. Bignozzi, B. Lenza, et al., Influence of natural patinas of outdoor quaternary bronzes on conservation treatments, Met. 2013, Proc. Interim Meet. ICOM-CC Met. Work. Gr. (2013), pp. 159–168.
[36] G. Masi, J. Esvan, C. Josse, C. Chiavari, E. Bernardi, C. Martini, et al., Characterization of typical patinas simulating bronze corrosion in outdoor conditions, Mater. Chem. Phys. 200 (2017) 308–321, https://doi.org/10.1016/j.matchemphys.2017.07.091.
[37] D.A. Scott, Copper and Bronze in art: corrosion, colorants, conservation, The Getty, Los Angeles (2002).
[38] F. Zanotto, V. Grassi, A. Frignani, F. Zucchi, Protection of the AZ31 magnesium alloy with cerium modified silane coatings, Mater. Chem. Phys. 129 (2011) 1–8.
[39] J. Bao, Q. Wang, X. Liu, L. Ding, Site-selective deposition of copper by controlling surface reactivity of SAMs with UV-irradiation, Surf. Sci. 602 (2008) 2250–2255, https://doi.org/10.1016/j.susc.2008.05.005.
[40] T. Kosec, D.K. Merl, I. Milošev, Impedance and XPS study of benzotriazole films formed on copper, copper-zinc alloys and zinc in chloride solution, Corros. Sci. 50 (2008) 1987–1997, https://doi.org/10.1016/j.corsci.2008.04.016.
[41] A. Galtayries, A. Mongiatti, P. Marcus, C. Chiavari, Surface characterisation of corrosion inhibitors on bronzes for artistic casting, Corros. Met. Herit. Artefacts Investig. Conserv. Predict. Long Term Behav. 48 (2007) 335–351, https://doi.org/10.1533/9781845693015.335.
[42] L. Tommesani, G. Brunoro, A. Frignani, C. Monticelli, M. Dal Colle, On the protective action of 1,2,3-benzotriazole derivative films ageinst copper corrosion, Corros Sci. 39 (1997) 1221–1237.
[43] F. Sinapi, S. Julien, D. Auguste, L. Hevesi, J. Delhalle, Z. Mekhalif, Monolayers and mixed-layers on copper towards corrosion protection, Electrochim. Acta 53 (2008) 4228–4238, https://doi.org/10.1016/j.electacta.2007.12.061.
[44] M. Finšgar, 2-Mercaptobenzimidazole as a copper corrosion inhibitor: part II. Surface analysis using X-ray photoelectron spectroscopy, Corros. Sci. 72 (2013) 90–98, https://doi.org/10.1016/j.corsci.2013.03.010.
[45] Z. Mekhalif, L. Massi, F. Guittard, S. Geribaldi, J. Delhalle, X-Ray Photoelectron Spectroscopy Study of Polycrystalline Zinc Modified By N -Dodecanethiol And 3-Perfluorooctyl-Propanethiol vol 405, (2002), pp. 186–193.
[46] F. Sinapi, I. Lejeune, J. Delhalle, Z. Mekhalif, Comparative protective abilities of organothiols SAM coatings applied to copper dissolution in aqueous environments, Electrochim. Acta 52 (2007) 5182–5190, https://doi.org/10.1016/j.electacta.2006.12.087.
[47] G.A. Bagiyan, I.K. Koroleva, N.V. Soroka, A.V. Ufimtsev, Oxidation of thiol compounds by molecular oxygen in aqueous solutions, Russ. Chem. Bull. 52 (2003) 1135–1141, https://doi.org/10.1023/A:1024761324710.
[48] W. Sui, W. Zhao, X. Zhang, S. Peng, Z. Zeng, Q. Xue, Comparative anti-corrosion properties of alkylthiols SAMs and mercapto functional silica sol-gel coatings on copper surface in sodium chloride solution, J. Solgel Sci. Technol. 80 (2016) 567–578, https://doi.org/10.1007/s10971-016-4108-y.
[49] G. Masi, A. Balbo, J. Esvan, C. Monticelli, J. Avila, L. Robbiola, et al., X-ray Photoelectron spectroscopy as a tool to investigate silane-based coatings for the protection of outdoor bronze: the role of alloying elements, Appl. Surf. Sci. 433 (2018), https://doi.org/10.1016/j.apsusc.2017.10.089.